EXOC4 Promotes Diffuse-Type Gastric Cancer Metastasis via Activating FAK Signal

Haojie Li[1], Xuhong Fu[2], Junjie Zhao[1], Chen Li[3,4], Lingmeng Li[2], Peiyan Xia[5], Jianping Guo[6], Wenyi Wei[7], Rong Zeng[3], Jiarui Wu[3], Yihong Sun[1], Liyu Huang[2], and Xuefei Wang[1]

ABSTRACT

In comparison with intestinal-type gastric cancer, diffuse-type gastric cancer (DGC) is more likely to recur, metastasize, and exhibit worse clinical outcomes; however, the underlying mechanism of DGC recurrence remains elusive. By employing an LC/MS-MS proteomic approach, we identified that exocyst complex component 4 (EXOC4) was significantly upregulated in DGC with recurrence, compared to those with nonrecurrence. High expression of EXOC4 was correlated with tumor metastasis and poor prognosis in patients with DGC. Moreover, EXOC4 promoted cell migration and invasion as well as the tumor metastasis of DGC cells. Mechanistically, EXOC4 regulated the phosphorylation of focal adhesion kinase (FAK) at Y397 sites by stimulating the secretion of integrin α5/β1/EGF and enhancing the interaction of FAK and integrin or EGFR. The FAK inhibitor VS-4718 reversed the metastasis mediated by *EXOC4* overexpression and suppressed the tumor growth of patient-derived xenografts derived from DGC with high EXOC4 expression. The EXOC4–FAK axis could be a potential therapeutic target for patients with DGC with high expression of EXOC4.

Implications: The EXOC4–FAK axis promoted DGC metastasis and could be a potential therapeutic target for patients with DGC.

Introduction

Gastric cancer remains one of the leading causes of cancer-related death, although its incidence has recently declined (1). In recent decades, the histologic classification of gastric cancer based on Lauren's criteria, which subdivides this cancer as intestinal-type, diffuse-type, and mixed-type gastric cancer, has been most commonly used to understand clinical diagnosis, prevention, and treatment (2). Diffuse-type gastric cancer (DGC) accounts for approximately 30% of gastric cancer cases, is more likely to affect younger people, and consists of individual infiltrating neoplastic cells without glandular structures, which contributes to its greater aggressiveness with a worst prognosis and few treatment options (3, 4). The 5-year survival rate of DGC is significantly lower than that of intestinal-type gastric cancer (IGC) due to the higher likelihoods of recurrence and peritoneal metastasis (5, 6). In comparison with well-studied IGC, which has been noted for a cascade involving *Helicobacter pylori* infection, inflammation, oxidative damage, atrophic gastritis, intestinal metaplasia, dysplasia, and ultimately gastric adenocarcinoma (7), DGC is known as an enigmatic disorder without well-defined precursor lesions or a carcinogenesis model. Specifically, DGC is characterized by highly malignant biological behaviors with prominent infiltration and poor cellular cohesion resulting in a high frequency of metastasis (5, 6, 8, 9). Thus, more thorough investigations are required to reveal the links between signaling pathways and metastasis and relapse in DGC. Ideally, an integrated proteogenomic analysis could generate a new paradigm for detecting proteomic alterations (10) and understanding the malignant biology of this cancer. In this study, a list of proteins differentially expressed between DGCs with and without recurrence was identified on the basis of proteogenomic analyses. Among the identified proteins, exocyst complex component 4 (EXOC4) was identified as a significantly upregulated protein in DGC samples with recurrence.

EXOC4, also known as Sec8, is a component of the exocyst complex that contributes to the tethering of secretory vesicles to the plasma membrane (11–13). The exocyst is an evolutionarily conserved hetero-octameric complex, and in mammalian cells, there are two exocyst subcomplexes consisting of EXOC1–EXOC2–EXOC3–EXOC4 (subcomplex I) and EXOC5–EXOC6–EXOC7–EXOC8 (subcomplex II; ref. 14). These two subcomplexes are recruited to vesicles independently and assemble into the holo-exocyst complex upon arrival at the plasma membrane, where the vesicles are tethered and fused (13, 14). A recent report discovered that exocysts are in dynamic equilibrium with

[1]Department of General Surgery, Zhongshan Hospital, General Surgery Research Institute, Fudan University, Shanghai, China. [2]Key Laboratory of Systems Biomedicine (Ministry of Education) and Collaborative Innovation Center of Systems Biomedicine, Shanghai Center for Systems Biomedicine, Shanghai Jiao Tong University, Shanghai, China. [3]Key Laboratory of Systems Biology, Institute of Biochemistry and Cell Biology, Shanghai Institutes for Biological Sciences, Chinese Academy of Sciences, Shanghai, China. [4]Center for Single-Cell Omics, School of Public Health, Shanghai Jiao Tong University School of Medicine, Shanghai, China. [5]University of Michigan-Shanghai Jiaotong University Joint Institute, Shanghai Jiao Tong University, Shanghai, China. [6]Institute of Precision Medicine, the First Affiliated Hospital, Sun Yat-sen University, Guangzhou, Guangdong, China. [7]Department of Pathology, Beth Israel Deaconess Medical Center, Harvard Medical School, Boston, Massachusetts.

Note: Supplementary data for this article are available at Molecular Cancer Research Online (http://mcr.aacrjournals.org/).

Haojie Li, Xuhong Fu, Junjie Zhao, and Chen Li contributed equally to this article.

Corresponding Authors: Xuefei Wang, Department of General Surgery, Zhongshan Hospital, Fudan University, 180 Fenglin Road, Shanghai 200032, China. Phone: 216-404-1990; Fax: 216-403-7224; E-mail: wang.xuefei@zs-hospital.sh.cn; Jiarui Wu, Key Laboratory of Systems Biology, Institute of Biochemistry and Cell Biology, Shanghai Institutes for Biological Sciences, Chinese Academy of Sciences, 320 Yueyang Road, Shanghai 200031, China. Phone: 212-030-5000; Fax: 212-032-5034; E-mail: wujr@sibs.ac.cn; Yihong Sun, Department of General Surgery, Zhongshan Hospital, Fudan University, 180 Fenglin Road, Shanghai 200032, China. Phone: 216-404-1990; Fax: 216-403-7269; E-mail: sun.yihong@zs-hospital.sh.cn; and Liyu Huang, Key Laboratory of Systems Biomedicine (Ministry of Education), Shanghai Center for Systems Biomedicine, Shanghai Jiao Tong University, 800 Dongchuan Road, Shanghai 200240, China. Phone: 213-420-7042; E-mail: huangly@sjtu.edu.cn

Mol Cancer Res 2022;20:1021–34

doi: 10.1158/1541-7786.MCR-21-0441

This open access article is distributed under the Creative Commons Attribution-NonCommercial-NoDerivatives 4.0 International (CC BY-NC-ND 4.0) license.

©2022 The Authors; Published by the American Association for Cancer Research

octamers and monomers (15). Every subunit may regulate cellular processes via the exocyst or independent of the exocyst complex. For example, during cell invasion, Exo70 (EXOC7), together with other exocyst components, participates in the secretion of matrix metalloproteinases. Furthermore, Exo70 interacts directly with the actin-related protein 2/3 complex independently of the holo-complex and stimulates actin branching, which in turn promotes invadopodia formation and cell invasion (16–18). Regarding Sec8 (EXOC4), in addition to its roles as a component of the exocyst and stimulating the secretion of neurotransmitters and cytokines, it has also been found to bind directly with c-JNK–interacting protein 4 to regulate MAPK signaling cascades in cervical cancer cells (19) and modulate TGFβ-induced EMT by regulating the expression of N-cadherin and Smad3/4 at the transcriptional level in lung cancer cells (20). However, the potential roles of EXOC4 in gastric malignancies remain largely unclear.

In this study, we revealed that EXOC4 is highly expressed in DGC and specifically correlated with recurrence and poor outcomes in patients with DGC. Mechanistically, EXOC4 could promote metastasis of DGC cells via activation of integrin/EGF-focal adhesion kinase $(FAK)^{Y397}$ signaling.

Materials and Methods

Patients

The study enrolled 444 patients with gastric cancer (including 127 DGC and 251 IGC) that had undergone a radical (R0) resection with a D2 lymphadenectomy from Zhongshan Hospital, Fudan University between 2004 and 2008. None of them received any neoadjuvant therapy. The demographic characteristics and the clinicopathologic parameters of each patient, including age, gender, tumor size, location, tumor differentiation, Lauren classification, vessel invasion, and TNM stage were retrospectively collected. Tumors and their adjacent normal tissues were collected within 30 minutes after operation, immediately transferred into liquid nitrogen, and then stored at –80°C until use. Tissues that were >60 mm away from the primary lesions were designated as normal mucosa tissues. Tumors and their adjacent normal tissues stained with hematoxylin and eosin (H&E) were evaluated by pathologists to confirm: (i) Lauren classification of tumors and (ii) no tumor cells in adjacent normal tissues. The study was approved by the ethics committee of Fudan University and was performed in accordance with the ethical standards laid down in the 1964 Declaration of Helsinki and its later amendments. Written informed consent was obtained from each patient.

Tissue microarrays and IHC

444 pairs of normal and tumor tissues were taken from enrolled patients, and then the validation of pathologic diagnosis using H&E staining of paraffin sections based on the 2010 World Health Organization classification system was conducted. For all samples, 2-mm cores were punched from the donor blocks and transferred to the recipient paraffin block at defined array positions. Several serial sections (4 μm in thickness) were cut from all tissue microarrays, and one of these was stained with H&E as a reference (21). For IHC staining, sections were incubated with EXOC4 antibody at a 1:100 dilution (Invitrogen, PA5–31027). Both the area and the intensity of immunopositive cells were used to evaluate the IHC staining. According to a previous study (22), the score was calculated by multiplying the staining area (0, <5%; 1, 5%–25%; 2, 26%–50%; 3, 51%–75%; and 4, >75%) and the intensity of the area (0, negative; 1, weak; 2, moderate; and 3, strong). The scores equal or higher than 4 were considered as high expression based on the area under the receiver operating characteristic curves and Youden index (Supplementary Table S1). Two pathologists who were blind to patients' clinical data in our hospital helped to assess the stained sections. The use of tissues and clinicopathologic data was approved by the ethics committee of Fudan University and was performed in accordance with the ethical standards laid down in the 1964 Declaration of Helsinki. Written informed consent was obtained from each patient.

Cells, antibodies, and reagents

Human gastric cancer cell lines HGC-27, MKN28, IM95, and AGS were from the Gastric Cancer Center of Fudan University; KATOIII and NUGC-4 were obtained from the Institute of Biochemistry and Cell Biology (Chinese Academy of Sciences); MKN45 and SNU-668 were purchased from Cobioer Biosciences Co., Ltd. All the cell lines obtained from the cell bank were tested for authentication using short tandem repeat fingerprinting and passaged for fewer than 6 months. Cells were cultured in DMEM or RPMI1640 supplemented with 10% FBS (catalog no. 16000–044; Gibco) at 37°C in a humidified atmosphere containing 5% CO_2. Cells were cultured according to the ATCC instructions and routinely tested to be negative for *Mycoplasma* contamination using the qPCR method (Thermo Fisher Scientific). The following antibodies were used: EXOC4 (Santa Cruz Biotechnology, catalog no. sc-136234, RRID:AB_2101573, 1:500), FAK (Cell Signaling Technology, #3283, 1:1,000), p-FAK (Tyr397;Cell Signaling Technology, #3285, 1:1,000), p-FAK (Tyr925;Cell Signaling Technology, #3284, 1:1,000), p-FAK (Tyr576/577;Cell Signaling Technology, #3281, 1:1,000), Erk (Cell Signaling Technology, #4695, 1:1,000), p-Erk (Thr202/Tyr204;Cell Signaling Technology, #4370, 1:1,000), Vimentin (Abcam, ab8978, 1:500), SNAI2 (Cell Signaling Technology, #9585, 1:1,000), SNAIL (Cell Signaling Technology, #3879, 1:1,000), GFP (Proteintech, 66002–1-Ig, 1:5,000), HA (Sigma, H6908, 1:1,000), ATP1A1 (Proteintech, 14418–1-AP, 1:1,000), Integrin α5 (Santa Cruz Biotechnology, sc-376199, 1:500), Integrin β1 (Santa Cruz Biotechnology, sc-374429, 1:500), EXOC3 (Santa Cruz Biotechnology, sc-374054, 1:200), EXOC5 (Proteintech, 17593–1-Ig, 1:500), and β-Tubulin (BPI, AbM59005–37B-PU, 1:5,000). The following chemotherapeutic reagents were used: EGF was purchased from Sigma-Aldrich; VS-4718 and gefitinib were purchased from MedChemExpress, ATN-161 (Ac-PHSCN-NH2) was manufactured by SelleckChem (S8454).

Proteomics analysis

Thirteen DGC samples were processed for proteomics analysis after excluding those with low DNA quality. All patients received 3-year follow-up every 6 months from the date of surgery. Recurrence was observed in four cases. The 13 DGC samples with their matched adjacent tissues were gathered, and combined with *in vitro* stable isotope labeling technique (dimethyl labeling) and LC/MS-MS analysis (23, 24) to look for potential biomarkers that were relative to prognosis. Protein sample preparation, digestion, and peptide labeling were performed according to previous reports (23–25). After peptide desalting by stage-tips, labeled peptide mixtures were prefractionated by high-pH RP column (26) on Dionex U3000 system (Thermo Fisher Scientific), and five fractions were obtained for each dimethyl labeling test. Each fraction was analyzed by nanoHPLC Orbitrap Velos (Thermo Fisher Scientific). MS raw files were analyzed by MaxQuant software (RRID:SCR_014485, version 1.3.2.8) and peak lists were searched against the human Uniprot FASTA database (downloaded in October, 2015). A total of 2,417 protein groups were identified and quantified with both protein and peptide FDR < 0.01. The proteomic

data have been uploaded to the National Omics Data Encyclopedia (NODE: OEP003074).

Pathway enrichment analysis

Gene-set enrichment analysis (GSEA) was used to identify enriched Kyoto Encyclopedia of Genes and Genomes (KEGG) pathway terms (RRID: SCR_012773, http://software.broadinstitute.org/gsea/index.jsp). The significance of fold enrichment was calculated using a $P < 0.05$ based on GSEA.

Lung metastasis mouse models

Study protocols involving mice were approved by the Institutional Animal Care and Use Committees of Shanghai Jiao Tong University. All sections of this report adhere to the Reporting of *In Vivo* Experiments (ARRIVE) guidelines. 5×10^6 luciferase-expressing MKN45 cells transduced with the indicated lentiviruses or plasmids were suspended in 200 μL of sterilized PBS and tail intravenously injected into male 6-week-old Balb/c nude mice or NOD-SCID mice. Then, the mice were randomly allocated to each group ($n = 5$–6) and orally administered with vehicle (control) or 50 mg/kg VS-4718 (MCE, HY-13917) per day for approximately 4 weeks. Mice were housed in individually ventilated cages with free access to water and food in a specific pathogen-free room. Lung metastasis was monitored periodically by injecting 100 μL of 15 mg/kg D-luciferin (YEASEN Biotechnology). After treatment for 30 days, all the mice were sacrificed by cervical dislocation after CO_2 inhalation.

Patient-derived xenograft mouse models

Fresh tumor samples (GAS190153, GAS190233, GAS190247, GAS190282, GAS190216, GAS190271) were collected from Chinese patients with gastric cancer undergoing gastrectomy at Zhongshan Hospital, Fudan University. All clinical sample collections were performed after obtaining informed consent from the corresponding patients and were approved by the ethics committees of Zhongshan Hospital. Tissue samples were sectioned into small pieces of approximately $2 \times 2 \times 2$ mm^3, and then were transplanted subcutaneously on the right dorsal flank of male 6-week-old NOD-SCID mice (Shanghai Lingchang Laboratory). Patients with different Lauren classification without preoperative chemoradiotherapy were selected to establish patient-derived xenograft (PDX) models, and xenografts were carried out within 3 to 5 hours following gastrectomy. A similar operation was performed to transfer the tumor piece to the next generation. After reaching generation 3 (P3), tumors were implanted subcutaneously on the right dorsal flank of 6-week-old NOD-SCID mice to do the *in vivo* experiment. The tumor volume was estimated as $(D \times d^2)/2$ (D, large diameter; d, small diameter). When the tumor volume reached 100 to 150 mm^3, FAK inhibitor (VS-4718, 50 mg/kg) or same volume of vehicle was administrated by intragastric injection once a day. Tumor volume and body weight were measured three times weekly. After treatment for approximately 4 weeks, all the mice were sacrificed by cervical dislocation after CO_2 inhalation, and the tumors were extracted, weighed, embedded in paraffin, and sectioned.

In vitro migration and invasion assay

Cell migration and invasion were measured by Transwell chambers (8-μm pores, Corning Life Sciences). Cells were transfected with indicated siRNA or plasmids before the migration and/or invasion assay. Afterwards, 1.5×10^5 cells were suspended in 100-μL serum-free medium and added on the membrane while DMEM containing 10% FBS (600 μL) was added into the bottom chamber. Cells incubated for 16 or 24 hours were fixed in 0.4% paraformaldehyde and stained with 0.1% crystal violet, then photographed by an optical microscope, and were then quantified in four independent fields in each sample. Data are shown as mean ± SD of three independent experiments.

RNA interference and plasmid transfection

RNA interference and plasmid transfection were performed with Lipofectamine 2000 (Invitrogen) according to the manufacturer's recommendations. The siRNAs (siRNA; GenePharma) used to deplete EXOC4 [siRNA#1: 5′-AAUCGACUAGCCGAGUUGUTT-3′; siRNA#2: 5′- CGACAGCCAUUCGCACAUATT-3′. For EXOC4, EXOC3, EXOC5 stable knockdown, short hairpin RNAs (shRNA; sense: shEXOC4: 5′-CCGGAGAACCTGCTTTCATGCAACTCGAG-TTGCATGAAAGCAGGTTCTTTTTTG-3′; shEXOC3: 5′-CCGGAC-AACGCCCTGAATGACGTCTCGAGACGTCATTCAGGGCGTTG-TTTTTTG-3′; shEXOC5: 5′-CCGGGCTCAGAAATTGATGAAATA-CCTCGAGGTATTTCATCAATTTCTGAGCTTTTTG-3′] were cloned into pLKO.1 vector. Plasmid pEGFP-EXOC4 was purchased from Addgene (#53758). For stable EXOC4 overexpression, full-length coding sequence (CDS) of EXOC4 was inserted into pCDH-copGFP vector and lentiviruses were packaged in 293T cells. PcDNA3-FAK-HA was obtained from Dr. Zeguang Han's lab (Shanghai Jiao Tong University, China). In addition, different fragments of EXOC4 and FAK were generated by subcloning the corresponding cDNAs into the pcDNA3-Flag-vector and the pcDNA3-HA-vector, respectively. The pcDNA3-ITGA5–3×Flag, pcDNA3-ITGB1–3×Flag, pcDNA3-ITGAV-3×Flag, and pcDNA3-ITGB3–3×Flag plasmids were constructed by Youbio Company.

Immunoprecipitation assay and Western blotting

When cells grew to 80% to 90% density in 10-mm dishes, then the cells were washed and lysed in immunoprecipitation buffer (50-mmol/L Tris, pH 8.0, 120-mmol/L NaCl, 0.5% NP-40) mixed with phosphatase inhibitors (phosphatase inhibitor cocktail set I and II, Bimake) and protease inhibitors (Complete Mini, Roche). For immunoprecipitation assay, 1 mg cell lysates were incubated with 2 μg specific antibodies at 4°C for 2 hours, and then added with preequilibrated protein-A Sepharose beads (Sigma). After incubation overnight at 4°C with gentle rotation, the immunocomplexes were then washed four times with NETN buffer (20 mmol/L Tris, pH 8.0, 100 mmol/L NaCl, 1 mmol/L EDTA, and 0.5% NP-40). After that, the bound proteins were eluted and subjected to Western blotting (WB). For WB assay, total proteins extracted from samples were separated by SDS-PAGE and transferred onto polyvinylidene difluoride membranes. The membranes were then incubated with specific antibodies, followed by secondary antibody and detected by enhanced chemiluminescence.

RT-PCR analysis

Total RNA was isolated using RNA Isolater Total RNA Extraction Reagent (Vazyme, R401–01), and reverse transcribed with HiScript II Q Select RT SuperMix (Vazyme, R223–01). Real-time PCR was performed using ChamQ Universal SYBR qPCR Master Mix (Vazyme, Q711–02) with Roche LightCycler96 system.

Phosphokinase antibody arrays

MKN45 cells were seeded in a 10-cm dish and transfected with siNC or siEXOC4#1 for 72 hours. Cells were lysed and 1 mg total protein was used to detect phosphorylation alteration by the Human Phospho-Kinase Antibody Array (#ARY003B, R&D Systems) following the manufacturer's instructions.

Immunofluorescence assay

Cells were treated as described previously and then were seeded on the glass coverslips, which were pretreated with Poly-L-Lysine

for the attachment of cell clusters. After attaching to the coverslips, cells were fixed in 0.4% paraformaldehyde and incubated with indicated antibodies according to the standard protocols. Fluorescence images were taken using a fluorescent confocal microscope (Nikon A1Si).

Statistical analysis

Statistical analysis was performed with SPSS (RRID:SCR_002865, version 19). Evaluation of *in vitro* and *in vivo* experiments was calculated using Student *t* test or one-way ANOVA. Kaplan–Meier survival curve and the log-rank test was used for survival analysis. All statistical analyses were two-sided, and $P < 0.05$ (*), $P < 0.01$ (**), and $P < 0.001$ (***), were considered statistically significant. Benjamini–Hochberg procedure was used to test for FDR.

Ethics approval

Tissue samples and clinicopathologic data were obtained from Zhongshan Hospital, Fudan University. Written informed consent from each patient was obtained. The research was approved by the Research Ethics Committee of Fudan University and was performed in accordance with the 1964 Declaration of Helsinki and its later amendments.

Data availability

The results shown here are in whole or part based upon data generated by The Cancer Genome Atlas (TCGA) Research Network (https://www.cancer.gov/tcga), Asian Cancer Research Group (ACRG) database (https://consortiapedia.fastercures.org/consortia/acrg/), and online Kaplan–Meier Plotter (http://www.kmplot.com/analysis/index.php?p=service&cancer=gastric). The proteomic data has been uploaded to the NODE: OEP003074. All the data supporting the findings of this study are available from the corresponding authors upon reasonable request.

Results

Proteomic screening identifies EXOC4 as a significant differentially expressed protein between recurrent and nonrecurrent DGC

To identify the key effectors that distinguish recurrent and nonrecurrent DGC, we initially analyzed 100 cases of DGC deposited in the tumor tissue bank of Zhongshan Hospital. After strict quality control of the tissue samples and accurate follow-up results, 13 DGC samples, including 9 samples from nonrecurrent patients and 4 samples from patients with recurrence within 3 years after surgery, were selected for proteomic profiling (Supplementary Table S2). Among the 2,417 proteins examined, 131 differentially expressed proteins ($P < 0.05$ and fold change >1.2, or $P < 0.05$ and fold change <0.8) were identified (**Fig. 1A** and **B**). Among these proteins, 103 proteins were upregulated ($P < 0.05$ and fold change >1.2) and 28 were downregulated ($P < 0.05$ and fold change <0.8) in DGC with recurrence compared with DGC without recurrence (**Fig. 1A** and **B**). We then submitted these altered proteins for KEGG-based enrichment analysis and found that among these 131 proteins, 29 proteins were involved in the tight junction pathway ($P = 0.016$; FDR q-value = 0.195) and showed the most significant changes (**Fig. 1C**). Because the tight junction pathway is closely related to cell adhesion, the permeability of the paracellular barrier, and tumor metastasis (27), we selected these 29 proteins for further expression analysis. We found that EXOC4 was the most upregulated protein in the recurrent DGC samples (**Fig. 1D**). In further support of this observation, we examined the TCGA database and found that DGC recurrence was more likely to occur in patients with high EXOC4 expression ($n = 19$) than in those with low EXOC4 expression ($n = 12$, $P = 0.032$; **Fig. 1E**). However, in IGC, EXOC4 expression was not indicative of tumor recurrence ($P = 0.425$; **Fig. 1E**). Other subunits of the exocyst (EXOC1, EXOC2, EXOC3, EXOC5, EXOC6, EXOC7, and EXOC8) were also analyzed in these datasets but were not found to be correlated with tumor recurrence in either DGC or IGC (Supplementary Fig. S1SA–S1G).

Therefore, these data suggest that EXOC4 is a specific biomarker of exocysts that indicates recurrence of DGC.

EXOC4 is highly expressed in DGC and correlates with poor outcomes of patients with DGC

To further evaluate the expression of EXOC4 in human gastric cancer, we first analyzed TCGA and ACRG databases, and found that EXOC4 expression was significantly elevated in tumor tissues ($n = 233$ in TCGA, and $n = 300$ in ACRG) compared with normal tissues ($n = 21$ in TCGA, and $n = 100$ in ACRG, $P < 0.001$; Supplementary Fig. S2A). In addition, we evaluated a large cohort of clinical samples from Zhongshan Hospital. The IHC results showed that EXOC4 protein expression was significantly increased in gastric tumors ($n = 444$, $P < 0.001$; Supplementary Fig. S2B). More interestingly, compared with IGC samples ($n = 251$ in Zhongshan cohort, and $n = 69$ in TCGA), EXOC4 expression was remarkably higher in DGC samples ($n = 127$ in Zhongshan cohort, and $n = 35$ in TCGA, $P < 0.001$; **Fig. 2A** and **B**). Meanwhile, other subunits of the exocyst did not show significant differences between DGC and IGC tissues, although most of these subunits demonstrated increased expression in whole tumor tissues compared with normal tissues (Supplementary Figs. S2C and S2D and S3A–S3G). Consistently, EXOC4 expression was much higher in DGC cell lines than in normal gastric epithelium GES-1 cells and IGC cell lines (**Fig. 2C**).

Moreover, we found that EXOC4 abundance was positively correlated with tumor infiltration ($P = 0.046$), lymph node metastasis ($P = 0.016$), and lymphatic vascular invasion (LVI; $P = 0.018$) in patients with DGC but not in patients with IGC (**Fig. 2D–F**; Supplementary Table S3). Specifically, the expression of EXOC4 in metastatic lymph nodes was dramatically higher than that in primary tumors ($P < 0.001$), indicating that tumor cells with high expression of EXOC4 might be prone to metastasis (**Fig. 2G**). Kaplan–Meier survival analyses demonstrated that patients with DGC with high EXOC4 expression ($n = 102$ in Zhongshan cohort, and $n = 65$ in GEO datasets) displayed lower overall survival than those with low EXOC4 expression ($n = 25$ in Zhongshan cohort, and $n = 65$ in GEO datasets, $P = 0.007$ and $P = 0.032$ respectively; **Fig. 2H** and **I**). However, survival differences associated with EXOC4 expression were not observed in patients with IGC ($P = 0.2457$; **Fig. 2H** and **I**). This prognostic specificity for DGC was not observed in other exocyst subunits (Supplementary Fig. S4A–S4G).

EXOC4 promotes DGC cell migration and metastasis

To analyze the biological function of EXOC4 in gastric cancer, we depleted *EXOC4* in the DGC cell lines MKN45 and SNU668 with siRNA or short hairpin RNA, respectively. As a result, reduced cell migration and invasion were observed in *EXOC4*-depleted DGC cells (**Fig. 3A** and **B**; Supplementary Fig. S5A and S5B). To further assess the physiologic roles of EXOC4 in regulating DGC cell metastasis, we engineered a distant metastasis mouse model by generating stable shScramble- and sh*EXOC4*-luciferase MKN45 cell lines. The results showed that *EXOC4* depletion could significantly decrease cancer cell lung metastasis (**Fig. 3C**). In contrast, EXOC4 overexpression in

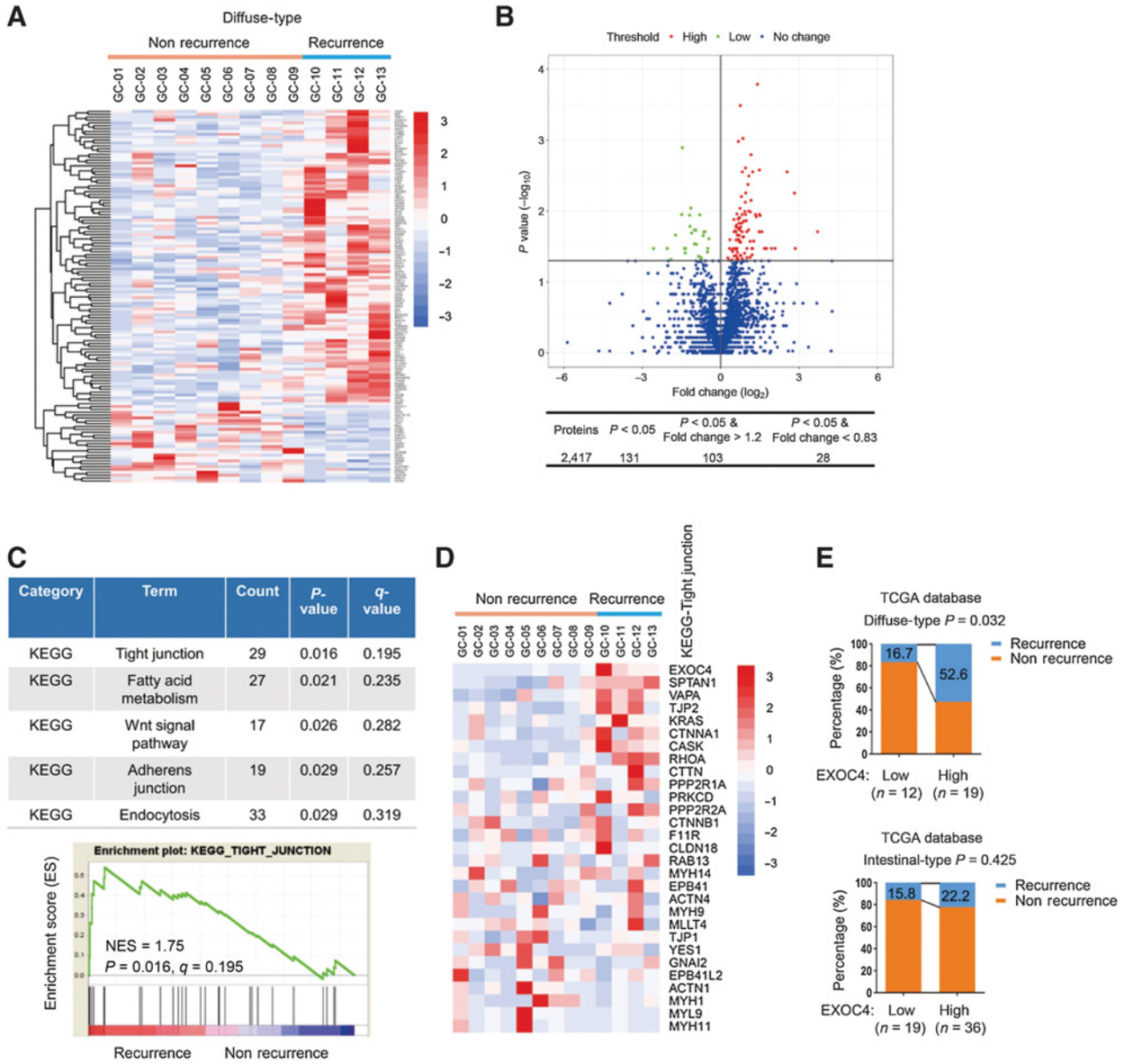

Figure 1.

Proteomic screening identifies EXOC4 as a significantly differentially expressed protein in DGC between recurrence and nonrecurrence. **A,** Hierarchical cluster analysis (HCA) of proteome data. The globe heatmap depicted the relative protein expression alteration between 9 cases from nonrecurrent patients with DGC and 4 cases from patients with DGC with recurrence within 3 years after surgery (log2-transformed). **B,** The volcano plot illustrated the fold change of differential expression proteins. 103 of upregulated proteins were shown in red, 28 of downregulated ones were shown in green, and insignificant proteins were shown in blue. **C,** KEGG pathway analysis of differential expression proteins between nonrecurrent and recurrent DGC (top), and GSEA indicated a significant enrichment in tight junction pathway (bottom). **D,** The globe heatmap depicted the relative protein expression alteration in tight junction pathway (log_2-transformed). **E,** The proportion of nonrecurrent and recurrent DGC (top) or IGC (bottom) patients in EXOC4 low or high expression group from TCGA database.

MKN45 and SNU668 cells significantly increased cell migration and invasion *in vitro*, as well as tumor lung metastasis *in vivo* ($n = 5$, $P < 0.05$; (**Fig. 3D–F**; Supplementary Fig. S5C).

To identify which domain of EXOC4 might contribute to the regulation of DGC cell metastasis, we constructed a series of truncated mutants of EXOC4 (**Fig. 3G**). The N-terminus (aa 1–142) containing a coiled-coil domain is implicated in protein interactions with other members of the exocyst complex (28). The middle region (aa 143–402) is conserved among other members of the exocyst complex and termed the "exocyst complex component". The C-terminal domain (aa 403–973) is an EXOC4-specific domain that was previously reported to be the PDZ-binding domain and to interact with SAP102, which is involved in the delivery of NMDARs to the cell surface in heterologous cells and neurons (29). In our study, we found that only reintroduction of full-length EXOC4, but not other truncated mutants, could fully rescue the decreased cell migration and invasion of *EXOC4*-depleted cells (**Fig. 3H** and **I**), indicating that full-length EXOC4 was necessary for the regulation of DGC metastasis.

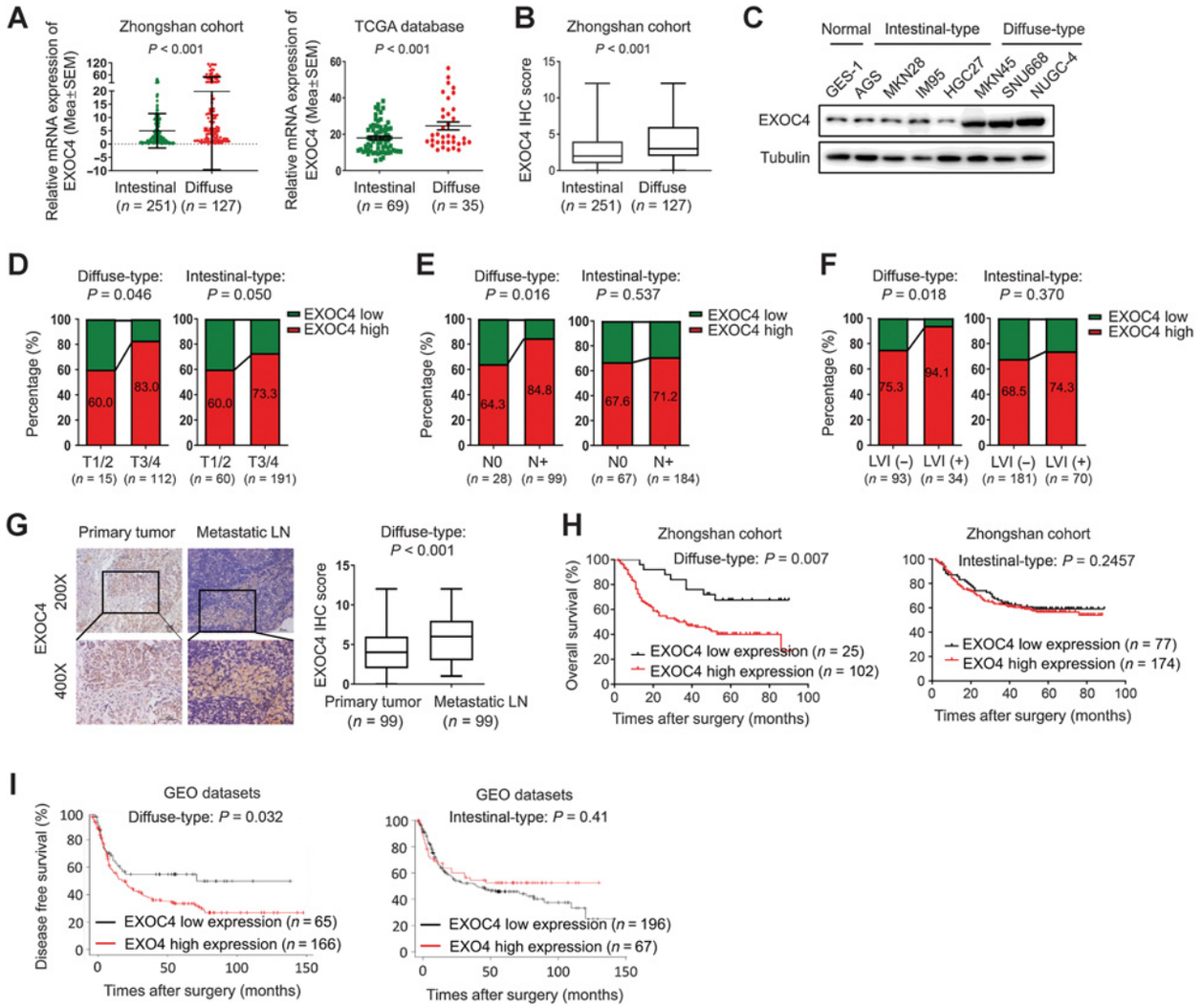

Figure 2.

EXOC4 is highly expressed in DGC and correlates with poor outcomes in patients with DGC. **A,** The expression of EXOC4 mRNA level in intestine and DGC from Zhongshan cohort and the TCGA database. **B,** The IHC staining scores of EXOC4 in IGC and DGCs. **C,** The expression of EXOC4 in different types of gastric cancer cell lines was examined by immunoblotting (IB). **D–F,** The proportion of EXOC4 high or low expression in different progressive stages of diffuse and intestine gastric cancer from Zhongshan cohort. T1/2, T stage I and II; T3/4, T stage III and IV; N0, no lymph node metastasis; N+, lymph node metastasis; LVI (-), no lymphovascular invasion; LVI (+), lymphovascular invasion. **G,** Representative images and scores of EXOC4 IHC staining in metastatic lymph node and primary tumor. Scale bar, 100 μm. **H,** Overall survival curve of patients with DGC and IGC with low or high expression of EXOC4 from Zhongshan cohort. **I,** Disease-free survival curve of patients with DGC and IGC with low or high expression of EXOC4 from the GEO database. Statistical significance was determined by two tailed unpaired Student *t* test (**A, B,** and **G**), Spearman rank correlation test (**D–F**) or log-rank test (**H** and **I**). GEO, Gene Expression Omnibus.

EXOC4 regulates FAK phosphorylation at Tyr397

To explore the potential underlying mechanism by which EXOC4 promotes DGC metastasis, we sought to determine the physiologic roles of EXOC4 in DGC. EXOC4 was previously reported to regulate cell migration by controlling ERK and p38 signaling in human oral squamous cell carcinoma (30). Therefore, we sought to determine which protein phosphorylation process or signaling pathway was affected by EXOC4 in DGC. On this premise, a human phosphokinase antibody array (catalog no. ARY003B, R&D Systems) was employed, and alterations in 43 phosphokinase sites that were likely crucial in the regulation of various cell processes, including cell migration and invasion, were evaluated. Among these phosphokinase sites, phospho–FAK-Tyr397 was the most remarkably changed in *EXOC4*-depleted MKN45 cells (**Fig. 4A** and **B**).

FAK is a well-established focal adhesion–associated kinase involved in cellular adhesion and spreading processes, and the phosphorylation of FAK-Tyr397 is largely involved in FAK activation, cell migration, and metastasis in many cancers (31, 32). To further verify the effect of EXOC4 expression on FAK phosphorylation in DGC cells, we measured the phosphorylation of FAK^{Y397} and observed that this event but not two other phosphorylation sites, $FAK^{Y576/577}$ and FAK^{Y925}, was significantly reduced upon *EXOC4* depletion in both MKN45 and SNU668 cells (**Fig. 4C**; Supplementary Fig. S6A). In contrast, p-FAK^{Y397} levels notably increased under EXOC4-overexpressing

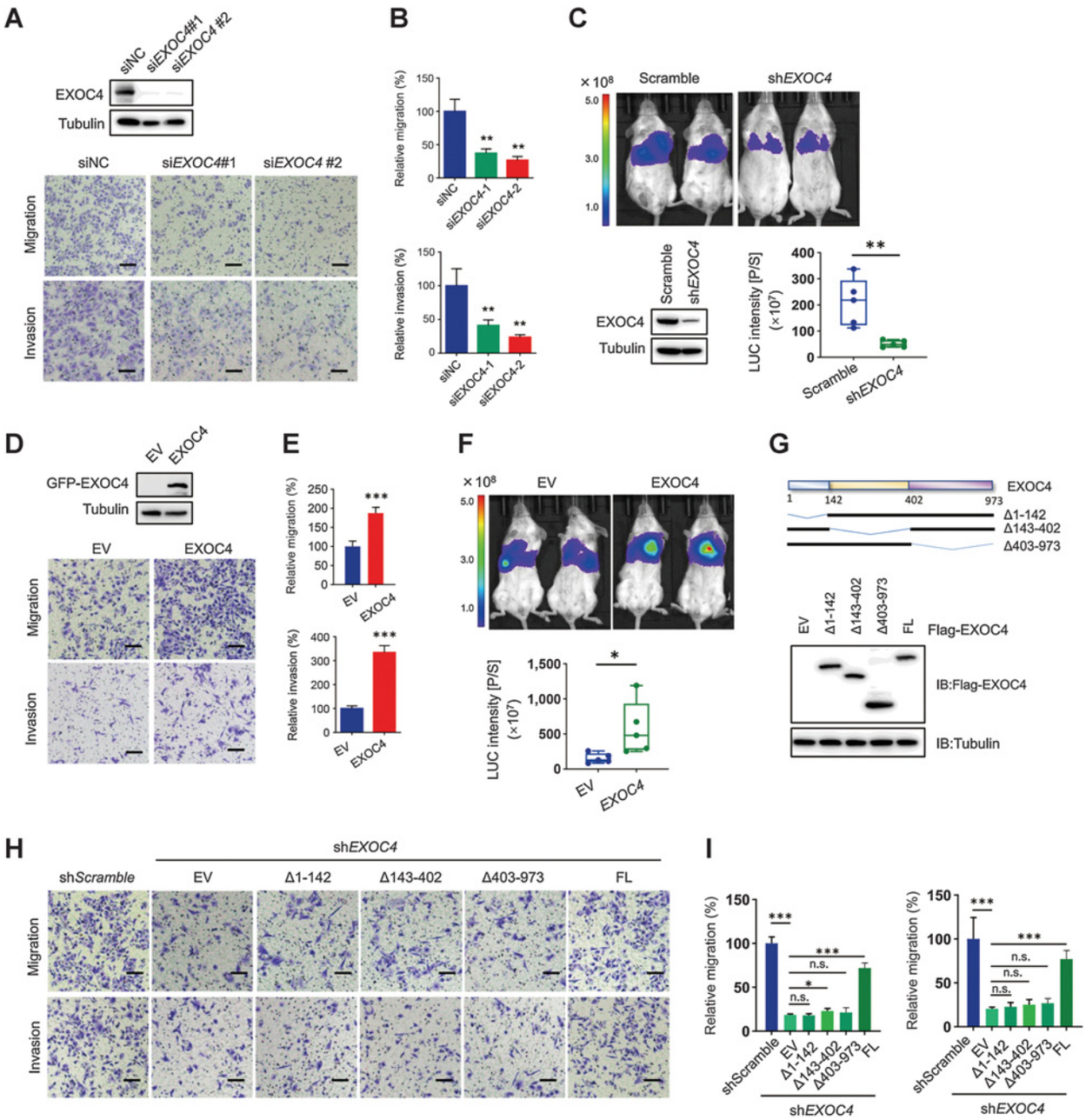

Figure 3.

EXOC4 promotes DGC cell migration and metastasis. **A** and **B,** Representative images (**A**) and the corresponding quantification (**B**) of migration and invasion of MKN45 cells infected with the indicated siRNA. Data were shown as mean ± SD of three independent experiments. **C,** Representative lung bioluminescence images (BLI) for MKN45-Scramble-Luciferase, MKN45-sh*EXOC4*-Luciferase cells, and quantification at day 30 ($n = 5$ per group). **D** and **E,** Representative images (**D**) and the corresponding quantification (**E**) of migration and invasion in MKN45 cells. Data were shown as mean ± SD of three independent experiments. **F,** Representative lung BLI for MKN45-EV-Luciferase, MKN45-EXOC4-Luciferase cells and quantification at day 30 ($n = 5$ per group). **G,** A schematic illustration of EXOC4 domain structures was shown on the upper panel. Immunoblotting (IB) analysis of whole-cell lysates (WCL) derived from 293T cells transfected with Flag-EXOC4 fragments was shown on the lower panel. **H** and **I,** MKN45-sh*EXOC4* cells were transfected with the indicated deletion variants or the full length of EXOC4 and then migration and invasion of cells were assayed by transwell assay. Data were shown as mean ± SD of three independent experiments. Statistical significance was determined by two-tailed unpaired Student *t* test: *, $P < 0.05$; **, $P < 0.01$; ***, $P < 0.001$. Scale bar, 100 μm. EV, empty vector.

conditions (**Fig. 4D**; Supplementary Fig. S6B). However, depletion of *EXOC3* or *EXOC5,* two other exocytosis-related proteins frequently involved in tumor progression (13, 14, 33), did not reduce FAK^{Y397}, FAK$^{Y576/577}$, or FAK^{Y925} phosphorylation in DGC cells (Supplementary Fig. S6C). Together, these findings strengthened the significance of EXOC4 in the regulation of the FAK signaling pathway.

Given that full-length EXOC4, but not the N-terminus of EXOC4, is involved in DGC malignancy, we hypothesize that more than the

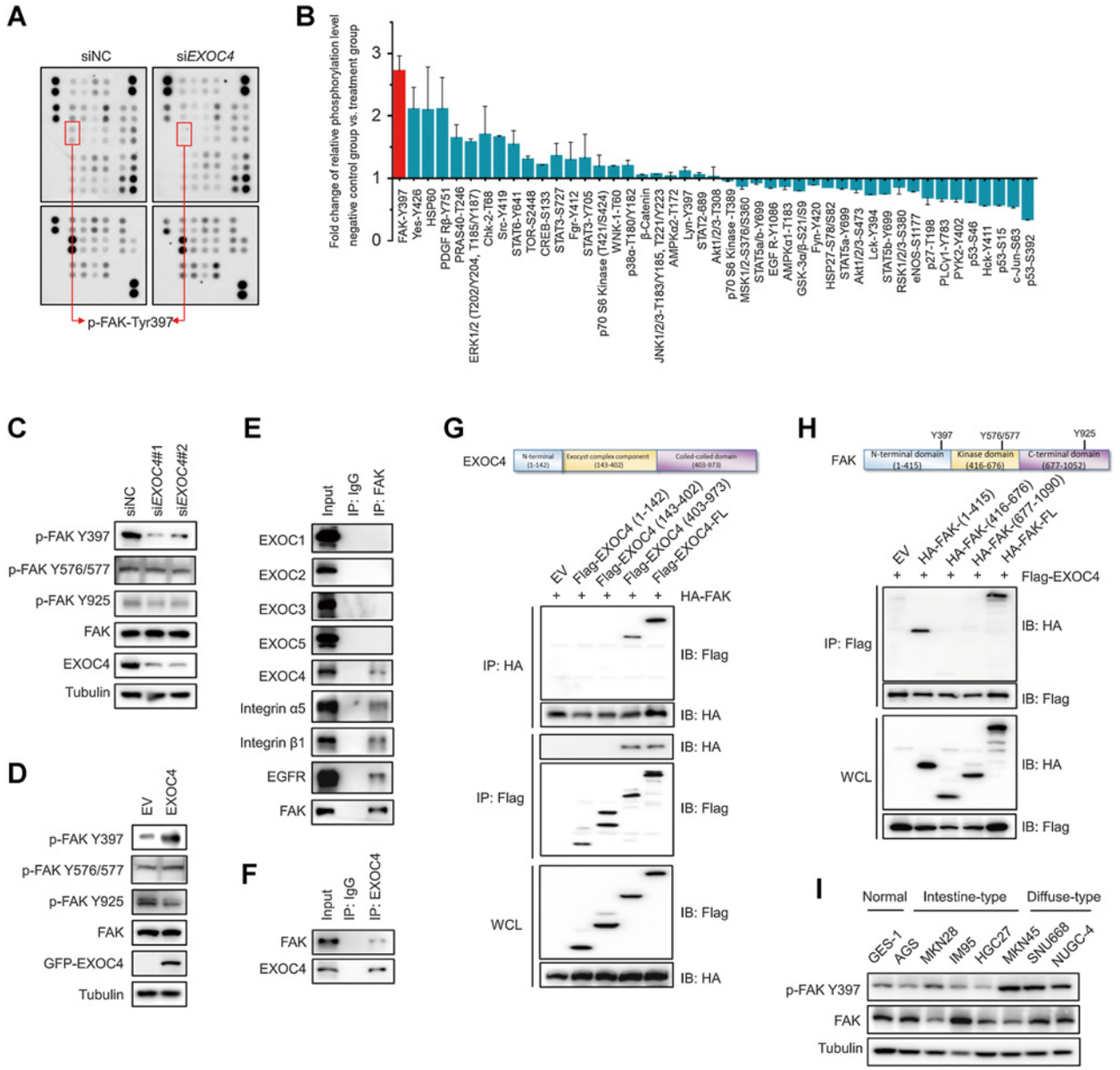

Figure 4.

EXOC4 regulates FAK phosphorylation at Tyr397. **A** and **B,** MKN45 cells were transfected with control or independent siRNAs against *EXOC4* for 48 hours and the WCLs were subjected to phosphokinase antibody array analysis (**A**), and the quantification were shown on (**B**). **C** and **D,** Immunoblotting (IB) analysis of whole-cell lysates (WCL) derived from MKN45 cells transfected with the indicated siRNA (**C**) or plasmids (**D**) for 48 hours. **E** and **F,** Co-IP experiments in MKN45 cells were performed using anti-FAK (**E**) or anti-EXOC4 (**F**) antibodies. IgG was used as a negative control. **G,** Co-IP analysis. IB analysis of WCLs and IPs derived from 293T cells transfected with HA-FAK together with the indicated Flag-tagged EXOC4. **H,** Co-IP analysis. IB analysis of WCLs and IPs derived from MKN45 cells transfected with Flag-EXOC4 together with the indicated constructs of HA-FAK. **I,** IB analysis of the FAK Y397 phosphorylation protein expression in different gastric cancer cells.

exocytosis-dependent roles of EXOC4 are involved in its pathologic functions. As such, we then conducted co-immunoprecipitation (co-IP) assays in DGC cells and 293T cells, and observed that FAK could bind to EXOC4 but not to other exocyst subunits, where EGFR and integrin were used as positive controls for binding with FAK (**Fig. 4E** and **F**; Supplementary Fig. S6D and S6E). In addition, we constructed different HA-tagged FAK protein fragments corresponding to the N-terminal domain (aa 1–415), kinase domain (aa 416–676), and C-terminal domain (aa 677–1090) of FAK. We found that FAK bound to the C-terminus of EXOC4 (aa 403–973), while EXOC4 bound to the N-terminal domain of FAK (aa 1–415), where FAK interacted with membrane receptors (**Fig. 4G** and **H**). Furthermore, we also examined FAK^{Y397} phosphorylation levels in different DGC cell lines and found that $p\text{-}FAK^{Y397}$ was higher in DGC cells than in normal gastric epithelial cells and IGC cells (**Fig. 4I**; ref. 34). IHC staining also demonstrated that the expression of p-FAK had a strong correlation with EXOC4 in DGC ($n = 127$, $r = 0.716$, $P < 0.001$; Supplementary Fig. S7A and S7B).

FAK inhibitor suppresses EXOC4-mediated DGC metastasis

To address whether EXOC4 promotes tumor metastasis by regulating FAK phosphorylation and activation in DGC cells, we introduced the wild-type (WT) form, or a phosphorylation-deficient mutant (Y397F) form of FAK, into *FAK*-depleted MKN45 cells and found that WT FAK but not Y397F FAK could promote MKN45 cell migration and invasion (**Fig. 5A–C**). Conversely, we introduced FAK-Y397E, a phosphomimetic mutation that retains sufficient biological activity dependent on upstream molecular activation, into *EXOC4*-depleted MKN45 cells and observed that FAK^{Y397E} but not FAK^{Y397F} could at least partially overcome the *EXOC4* depletion–induced reductions in DGC cell migration and invasion (**Fig. 5D** and **E**).

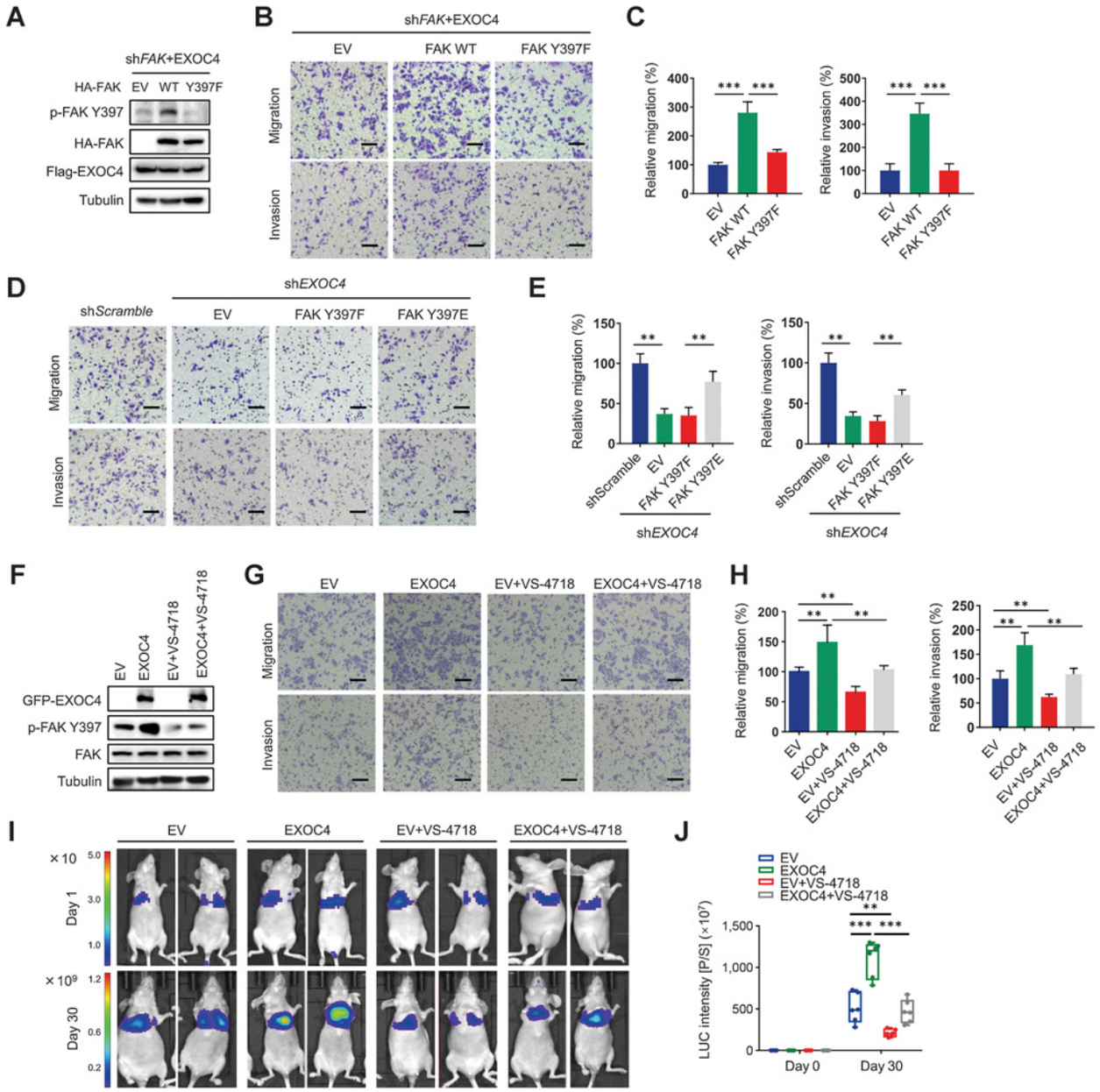

Figure 5.

FAK inhibitor suppresses EXOC4-mediated DGC metastasis. **A,** MKN45-sh*FAK* cells were infected with Flag-EXOC4, WT or mutant HA-FAK (Y397F) plasmids and then were harvested for IB analysis. **B–E,** Representative images (**B** and **D**) and the corresponding quantification (**C** and **E**) of transwell assay of MKN45 cells transfected with the indicated plasmids. **F,** MKN45 cells were infected with the indicated plasmids, treated with or without FAK inhibitor (VS-4718, 1 μmol/L, 24 hours) and then were harvested for immunoblotting (IB) analysis. **G** and **H,** Representative images (**G**) and the corresponding quantification (**H**) of transwell assay of MKN45 cells treated as indicated in (**F**). **I** and **J,** Representative lung bioluminescence images (BLI) for MKN45-Luciferase and MKN45-EXOC4-Luciferase cells with or without VS-4718 treatment (50 mg/kg/day, i.g.) at day 0 (top) and day 30 (bottom; **I**) and the quantification (**J**; $n = 6$ per group). Data were shown as mean ± SD of three independent experiments. Statistical significance was determined by two-tailed unpaired Student *t* test: *, $P < 0.05$; **, $P < 0.01$; ***, $P < 0.001$. Scale bar, 100 μm.

Next, we used the FAK kinase inhibitor VS-4718, a novel selective FAK tyrosine kinase inhibitor, that has been evaluated as a cancer therapy in clinical trials (35, 36), to treat EXOC4-overexpressing DGC cells. The results showed that VS-4718 remarkably reduced the increased cell migration and invasion mediated by EXOC4 overexpression in MKN45 and SNU668 cells (**Fig. 5F–H**; Supplementary Fig. S8A and S8B). Furthermore, VS-4718 significantly suppressed MKN45 cell lung metastasis mediated by EXOC4 overexpression in a nude mouse model ($n = 6$, $P < 0.001$; **Fig. 5I** and **J**; Supplementary Fig. S8C). These findings indicate that FAK may be a potential therapeutic target in patients with DGC with high *EXOC4* expression.

EXOC4 stimulates the secretion of integrin α5/β1 and EGF and enhances the interaction of FAK with membrane receptors

As a component of the exocyst, EXOC4 can assist in the docking of secretory vesicles to the plasma membrane and promote the release of secretory proteins by vesicles (11, 13). Therefore, we intended to determine whether EXOC4 affected the secretion or activation of FAK upstream factors, such as integrin α5/β1 and EGF, which are directly related to FAK phosphorylation (35, 37), in DGC cells. We first examined the concentrations of integrin α5 and EGF in the serum of patients with DGC by ELISA. We found that both serum integrin α5 and EGF levels were remarkably higher in patients with DGC with lymph node metastasis (N+, $n = 99$) than in patients without metastasis (N0, $n = 28$, $P < 0.001$ and $P = 0.0094$ respectively; **Fig. 6A**). More interestingly, we observed that the expression level of EXOC4 was positively correlated with the serum concentrations of integrin α5 and EGF in these DGC samples ($P < 0.001$; **Fig. 6B**). To investigate the secretory roles of EXOC4, we enriched vesicles derived from MKN45 cells and 293T cells by density gradient centrifugation and found that EXOC4 could promote the secretion of vesicles carrying both integrin α5/β1 and EGF (**Fig. 6C–E**). Consistent with these findings, FAK signaling, including the phosphorylation of FAK^{Y397} and $ERK^{T202/Y204}$, was significantly activated in cells cultured with EXOC4-overexpressing cell conditioned medium; serum-free medium was used as a negative control, and 10% FBS medium was used as a positive control (**Fig. 6F**).

It is well established that FAK is recruited to sites of integrin clustering and interacts with integrin-associated proteins through its C-terminal domain, leading to FAK activation (38, 39). In addition, FAK can be stimulated by EGF and interacts with activated EGFR through its N-terminal domain, which has an important function in promoting EGF-stimulated cell migration (35, 38). Because EXOC4 could directly bind with FAK (**Fig. 4**), we sought to determine whether EXOC4 modulated the interactions of FAK and upstream signaling effectors directly. Interestingly, our co-IP results showed that the interactions of FAK with integrin/EGFR were significantly enhanced upon EXOC4 overexpression and could not be abolished by the EGFR inhibitor gefitinib or the anti-integrin peptide ATN-161 (**Fig. 6G–I**). Furthermore, we found that the integrin peptide antagonist ATN-161 could efficiently overcome EXOC4 overexpression–induced MKN45 cell migration and invasion (**Fig. 6J** and **K**; Supplementary Fig. S8D). On the other hand, the activated FAK signaling, increased cell migration, and invasion triggered by EGF could be markedly repressed by depleting *EXOC4* in MKN45 cells (**Fig. 6L** and **M**; Supplementary Fig. S8E).

Together, these data indicate that EXOC4 can positively regulate FAK signaling by both stimulating integrin/EGF secretion and enhancing the interactions of FAK with its upstream effectors, highlighting the potential of a strategy of targeting FAK signaling to combat EXOC4 overexpression–mediated DGC metastasis.

A FAK inhibitor suppresses the growth of the PDXs derived from DGC or mixed-type gastric cancer with high EXOC4 expression

We next tested the therapeutic potential of the FAK inhibitor VS-4718 in different PDX models derived from human gastric cancers. Six patients with different Lauren classifications without preoperative chemoradiotherapy were selected to establish PDX models, of which two samples were DGC (GAS190153 and GAS190233), two samples were mixed-type gastric cancer (GAS190247 and GAS190282), and two samples were IGC (GAS190216 and GAS190271). We verified the expression of EXOC4 and $p\text{-}FAK^{Y397}$ in the gastric cancer samples (**Fig. 7A** and **B**; Supplementary Fig. S9A) and then treated the PDX models derived from these samples with VS-4718. Approximately 3 to 4 weeks later, we found that the VS-4718 could markedly reduce tumor growth in the four $EXOC4^{high}$ PDX models ($P < 0.01$) but had no significant effect on the $EXOC4^{low}$ IGC xenograft models (**Fig. 7C**; Supplementary Fig. S9B–S9E). Accordingly, the expression of the proliferation marker Ki67 was significantly reduced in the PDX models with high EXOC4 expression when treated with VS-4718 (**Fig. 7D**); however, a similar result was not observed in IGC with low EXOC4 expression (**Fig. 7E**). These results suggest that FAK inhibitors may have a therapeutic effect on patients with human gastric cancer with high EXOC4 expression.

Discussion

As a complex and highly heterogeneous disease, gastric cancer has been grouped by different biological and clinical features with unclear molecular mechanisms (5, 40). With the rapid development of multiomic technology, unidentified molecular factors in DGC are being revealed, including their impacts on clinical outcomes (41). Recent research results from TCGA and the ACRG have shown that DGC is predominantly found within the genomically stable group and microsatellite stable group with an overall poor prognosis, characterized by mutations in *CDH1*, *TP53*, *RHOA*, *CTNN1A*, *CMTM2,* and *CLDN18-ARHGAP* fusion (42). Conceivably, genomic alterations in adhesion and motility proteins in DGC may also contribute to its infiltrative and poorly cohesive histology. Zhang and colleagues recently reported that $RHOA^{Y42C}$ with inactivation of the canonical tumor suppressor *Cdh1* induced metastatic DGC in a mouse model (34). The authors revealed how the $RHOA^{Y42C}$ mutation mediates FAK activation and imparts sensitivity to pharmacologic FAK inhibitors in DGC (34). In this study, by using a proteomics-based approach, we found that the expression of EXOC4, a component of the exocyst, was highly increased in DGC samples with tumor recurrence compared with nonrecurrent samples. Analysis of the TCGA database also validated the association of high EXOC4 expression with DGC recurrence, which indicated the value of EXOC4 as a potential predictive marker for DGC recurrence in patients after surgery.

The exocyst is a conserved octameric protein complex that tethers secretory vesicles during exocytosis and is implicated in multiple cellular processes, such as secretion, membrane transduction, cytokinesis, autophagy, and ciliogenesis (11, 15). Under pathologic conditions and specifically in the gastric cancer setting, the role of the exocyst has not been investigated previously. In this study, we showed that EXOC4, but not other components of the exocyst, played specific and significant roles in DGC metastasis and recurrence. More significantly, we first demonstrated that EXOC4 could stimulate the activation of FAK in DGC cells via the role of exocyst or independent of the holo–exocyst complex. On one hand, EXOC4 could directly bind with FAK, assisting FAK to move from cytoplasm to cell membrane and enhancing its interactions with the upstream integrin α5/β1 receptor and

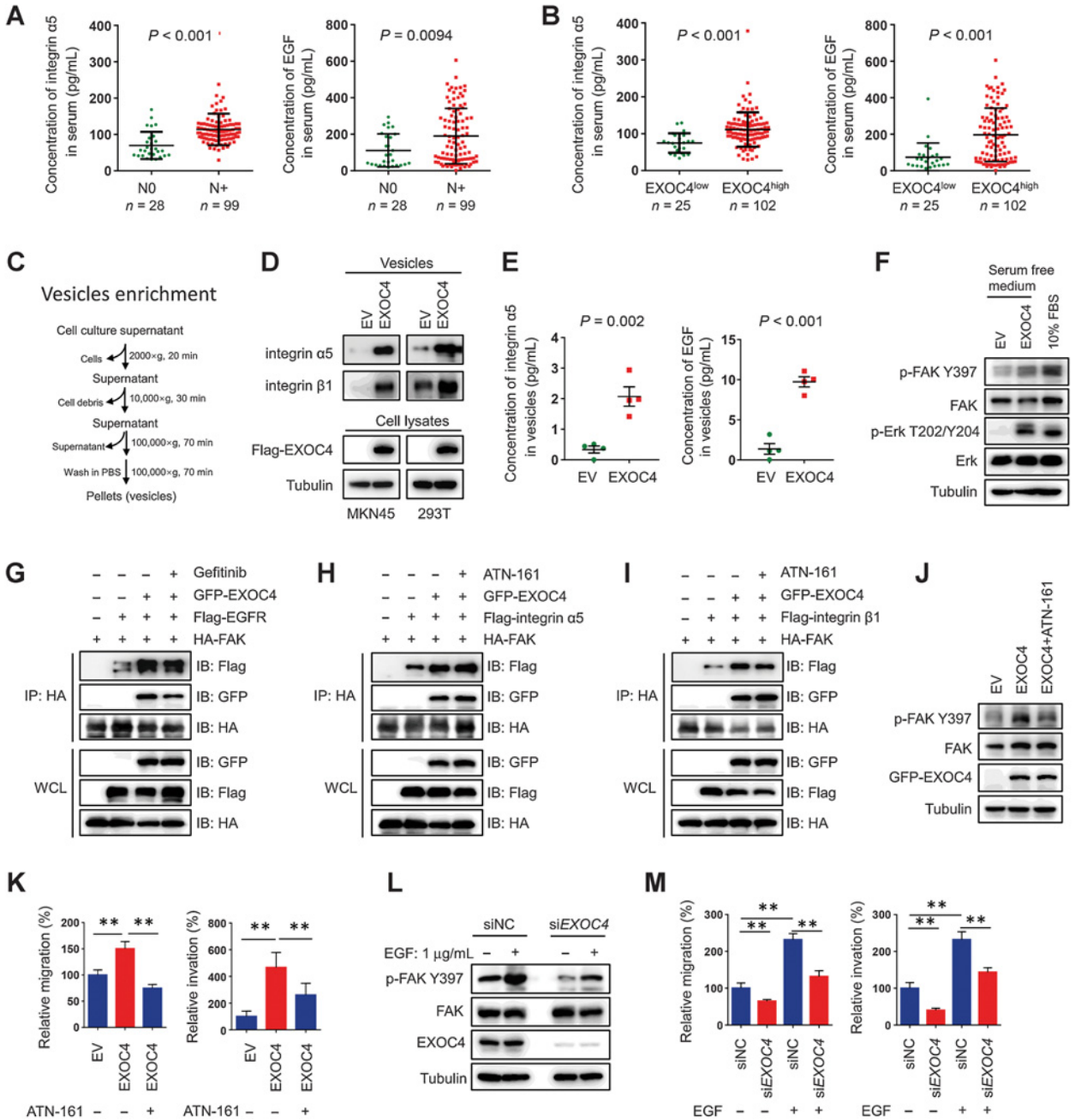

Figure 6.

EXOC4 stimulates the secretion of integrin α5/β1 and EGF and enhances the interaction of FAK with the integrin/EGF receptor. **A** and **B,** Concentration of integrin α5 and EGF in gastric cancer patients' serum. ELISA assay was used to detect integrin α5 and EGF in 28 cases with no lymph node metastasis (N0) and 99 cases with lymph node metastasis (N+; **A**) or in 25 cases with low EXOC4 expression and 102 cases with high EXOC4 expression (**B**). **C,** Schematic representation of vehicles enrichment. **D,** Immunoblotting (IB) analysis of vesicles collected as indicated in (**C**) and corresponding cell lysates from MKN45 and 293T cells transfected with lentivirus encoding either empty vector (EV) or Flag-tagged EXOC4. **E,** Vesicles enriched from MKN45-EV or MKN45-EXOC4 were used for ELISA analysis of integrin α5 and EGF. **F,** IB analysis of starved MKN45 cells cultured with the indicated medium (serum-free medium; EXOC4-overexpressing cell conditioned medium; 10% FBS medium) respectively for 48 hours, then WCLs were collected and tended to IB analysis. **G–I,** IB analysis of WCLs and immunoprecipitations derived from 293T cells transfected with indicated plasmids. **J,** IB analysis of MKN45 cells transfected with the indicated proteins with or without ATN-161 treatment. MKN45 cells were transfected with EV or GFP-tagged EXOC4 plasmids for 48 hours and then were treated with or without 10 μmol/L ATN-161 for 24 hours. **K,** Transwell assay of MKN45 cells infected with the indicated plasmids and treated with 10 μmol/L ATN-161. **L,** IB analysis of MKN45 cells transfected with the indicated siRNA and treated with 1 μg/mL EGF. **M,** Transwell assay of MKN45 cells transfected with the indicated siRNA. Data were shown as mean ± SD of three independent experiments. Statistical significance was determined by two-tailed unpaired Student *t* test: **, $P < 0.01$.

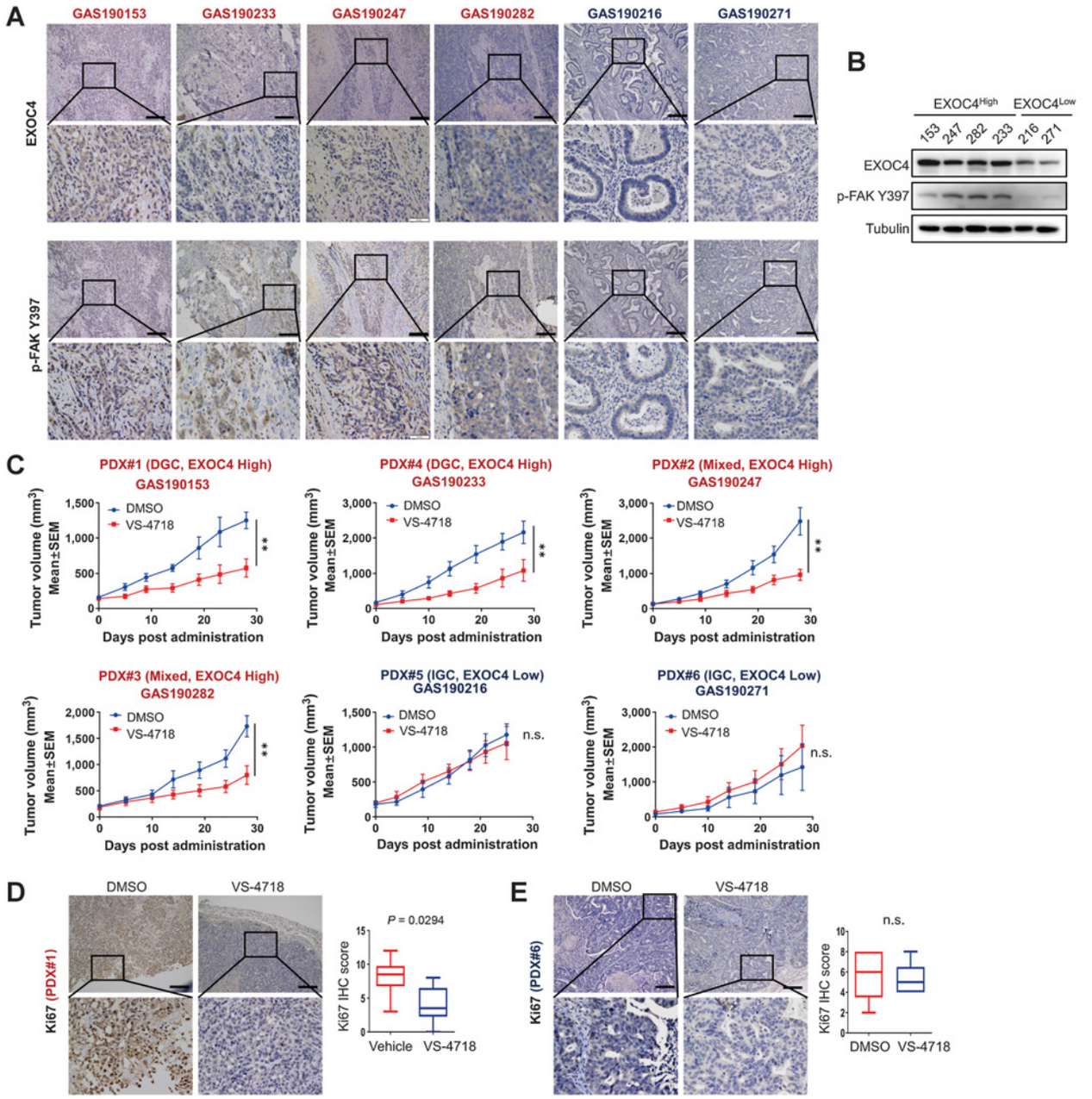

Figure 7.

FAK is a potent therapeutic target for patients with human gastric cancer with high EXOC4 expression. **A,** IHC staining of EXOC4 and p-FAK Y397 in six PDX models (GAS190153, DGC; GAS190233, DGC; GAS190247, Mixed-type gastric cancer; GAS190282, Mixed-type GC; GAS190216, IGC; GAS190271, IGC). Scale bar, 200 μmol/L. **B,** IB analysis of EXOC4 and p-FAK^{Y397} expression in six PDX samples. **C,** The tumor growth curves of six PDX were shown as indicated. Tumors from PDX models were injected subcutaneously into the dorsal flank of 6-week-old NOD/SCID mice. FAK inhibitor (VS-4718, 50 mg/kg) or DMSO was administrated by intragastric injection. **, $P < 0.01$; n.s., nonsignificant. **D** and **E,** Representative images and scores of Ki67 staining in DMSO and VS-4718 treatment group were shown in **D** (PDX#1, DGC), and in **E** (PDX#5, IGC). Scale bar, 200 μmol/L. Data were shown as mean ± SEM of three independent experiments. Statistical significance was determined by two-tailed unpaired Student *t* test: n.s., nonsignificant.

EGFR (Supplementary Fig. S10). On the other hand, EXOC4 could stimulate the secretion of FAK upstream effectors such as integrin α5/β1 and EGF in an exocyst-dependent manner and this correlated with elevated serum levels of integrin α5/β1/EGF in patients with DGC. Through these two different processes, EXOC4 markedly facilitates FAK phosphorylation at Tyr397, enhancing FAK kinase activity and contributing to DGC cell invasion, migration, and metastasis (Supplementary Fig. S10).

To validate our findings, we also employed FAK inhibitors and integrin antagonist peptides, which significantly repressed EXOC4-mediated DGC malignancy *in vitro* and *in vivo*. More significantly, we evaluated the therapeutic effect of the FAK inhibitor VS-4718 in PDX

models derived from human gastric cancers. The results highlighted the potential of a strategy targeting FAK for high EXOC4 expression DGC cancer therapies. Although the result was promising, it also indicated that FAK inhibitor might need combination therapy as all of the PDXs continued to grow, albeit less than control, while on VS-4718. For one reason, EXOC4 may have other biological function to regulate tumor growth and metastasis in DGC, which need to be further explored. For another reason, gastric cancer is recognized as a complex and multifactorial disease that is associated with a wide range of molecular mechanism. As such, except for FAK, other genes or signaling may contribute to tumorigenesis of DGC.

There are certainly limitations of our study. First, the number of patients for proteomic screening is small, so there could be selection bias here, and the different recurrence pattern has not been compared. Moreover, how EXOC4 is upregulated in gastric cancer, especially in DGC, is not clarified. Then, the relationship between EXOC4 and several well-known DGC-associated genes, like *CDH1*, and RHOA has yet to uncover. Next, this study focuses on the function of EXOC4 itself. However, as a component of exocyst, how exocyst contributes to metastasis of gastric cancer has not been discovered. Finally, the inhibitor against EXOC4 is not developed to demonstrate the therapeutic effect targeting EXOC4 in DGC, which will be further explored in our future direction.

In conclusion, our findings not only identify a molecular mechanism for DGC recurrence via EXOC4–integrin α5/β1/EGF–FAK signaling, but also provide a promising target for the treatment of patients with DGC with high EXOC4 expression.

Authors' Disclosures

No disclosures were reported..

Authors' Contributions

H. Li: Data curation, formal analysis, writing–original draft. **X. Fu:** Data curation, software, formal analysis, investigation, methodology, writing–original draft. **J. Zhao:** Data curation, formal analysis, methodology, writing–original draft. **C. Li:** Resources, software, formal analysis. **L. Li:** Software, validation, methodology. **P. Xia:** Software, formal analysis. **J. Guo:** Project administration, writing–review and editing. **W. Wei:** Visualization, methodology. **R. Zeng:** Resources, data curation, software, supervision, methodology. **J. Wu:** Conceptualization, resources, data curation, software. **Y. Sun:** Conceptualization, funding acquisition, writing–review and editing. **L. Huang:** Resources, data curation, funding acquisition, writing–review and editing. **X. Wang:** Conceptualization, resources, validation.

Acknowledgments

We thank Dr. Rongkui Luo (Department of Pathology, Zhongshan Hospital, Fudan University, Shanghai, China) for his kind help in evaluation, IHC staining, and Lauren classification of tissue microarrays. This work was supported in part by the National Natural Science Foundation of China (to Y. Sun; 81872425; to X. Wang 81972228; and L. Huang, 81872346), and Shanghai Pu Jiang Talents plan (to X. Wang, 2019PJD005).

The costs of publication of this article were defrayed in part by the payment of page charges. This article must therefore be hereby marked *advertisement* in accordance with 18 U.S.C. Section 1734 solely to indicate this fact.

Received June 9, 2021; revised December 1, 2021; accepted March 17, 2022; published first April 26, 2022.

References

1. Bray F, Ferlay J, Soerjomataram I, Siegel RL, Torre LA, Jemal A. Global cancer statistics 2018: GLOBOCAN estimates of incidence and mortality worldwide for 36 cancers in 185 countries. CA Cancer J Clin 2018;68:394–424.
2. Lauren P. The two histological main types of gastric carcinoma diffuse and so-called intestinal-type carcinoma. An attempt at a histo-clinical classification. Acta Pathol Microbiol Scand 1965;64:31.
3. Kakiuchi M, Nishizawa T, Ueda H, Gotoh K, Tanaka A, Hayashi A, et al. Recurrent gain-of-function mutations of RHOA in diffuse-type gastric carcinoma. Nat Genet 2014;46:583–7.
4. Cho SJ, Yoon C, Lee JH, Chang KK, Lin JX, Kim YH, et al. KMT2C mutations in diffuse-type gastric adenocarcinoma promote epithelial-to-mesenchymal transition. Clin Cancer Res 2018;24:6556–69.
5. Chen YC, Fang WL, Wang RF, Liu CA, Yang MH, Lo SS, et al. Clinicopathologic variation of Lauren classification in gastric cancer. Pathol Oncol Res 2016;22:197–202.
6. Marrelli D, Roviello F, de Manzoni G, Morgagni P, Di Leo A, Saragoni L, et al. Different patterns of recurrence in gastric cancer depending on Lauren's histological type: longitudinal study. World J Surg 2002;26:1160–5.
7. Holmes K, Egan B, Swan N, O'Morain C. Genetic mechanisms and aberrant gene expression during the development of gastric intestinal metaplasia and adenocarcinoma. Curr Genomics 2007;8:379–97.
8. Inokuchi M, Murase H, Otsuki S, Kawano T, Kojima K. Different clinical significance of FGFR1–4 expression between diffuse-type and intestinal-type gastric cancer. World J Surg Oncol 2017;15:2.
9. Yoon C, Cho SJ, Aksoy BA, Park DJ, Schultz N, Ryeom SW, et al. Chemotherapy resistance in diffuse-type gastric adenocarcinoma is mediated by RhoA activation in cancer stem-like cells. Clin Cancer Res 2016;22:971–83.
10. Rodriguez H, Pennington SR. Revolutionizing precision oncology through collaborative proteogenomics and data sharing. Cell 2018;173:535–39.
11. Mei K, Guo W. The exocyst complex. Curr Biol 2018;28:R922–R25.
12. Martin-Urdiroz M, Deeks MJ, Horton CG, Dawe HR, Jourdain I. The exocyst complex in health and disease. Front Cell Dev Biol 2016;4:24.
13. Torres MJ, Pandita RK, Kulak O, Kumar R, Formstecher E, Horikoshi N, et al. Role of the exocyst complex component Sec6/8 in genomic stability. Mol Cell Biol 2015;35:3633–45.
14. Tanaka T, Goto K, Iino M. Diverse functions and signal transduction of the exocyst complex in tumor cells. J Cell Physiol 2017;232:939–57.
15. Ahmed SM, Nishida-Fukuda H, Li Y, McDonald WH, Gradinaru CC, Macara IG. Exocyst dynamics during vesicle tethering and fusion. Nat Commun 2018;9:5140.
16. Liu J, Yue P, Artym VV, Mueller SC, Guo W. The role of the exocyst in matrix metalloproteinase secretion and actin dynamics during tumor cell invadopodia formation. Mol Biol Cell 2009;20:3763–71.
17. Zuo X, Zhang J, Zhang Y, Hsu SC, Zhou D, Guo W. Exo70 interacts with the Arp2/3 complex and regulates cell migration. Nat Cell Biol 2006;8:1383–8.
18. Liu J, Zhao Y, Sun Y, He B, Yang C, Svitkina T, et al. Exo70 stimulates the Arp2/3 complex for lamellipodia formation and directional cell migration. Curr Biol 2012;22:1510–5.
19. Tanaka T, Iino M, Goto K. Knockdown of Sec8 enhances the binding affinity of c-Jun N-terminal kinase (JNK)-interacting protein 4 for mitogen-activated protein kinase kinase 4 (MKK4) and suppresses the phosphorylation of MKK4, p38, and JNK, thereby inhibiting apoptosis. FEBS J 2014;281:5237–50.
20. Tanaka T, Goto K, Iino M. Sec8 modulates TGFβ–induced EMT by controlling N-cadherin via regulation of Smad3/4. Cell Signal 2017;29:115–26.
21. Min L, Ruan Y, Shen Z, Jia D, Wang X, Zhao J, et al. Overexpression of Ras-GTPase–activating protein SH3 domain-binding protein 1 correlates with poor prognosis in gastric cancer. Histopathology 2015;67:677–88.
22. Zhao J, Li H, Min L, Han X, Shu P, Yang Y, et al. High expression of tumor necrosis factor receptor—associated factor 2 promotes tumor metastasis and is associated with unfavorable prognosis in gastric cancer. J Gastroenterol Hepatol 2018;33:431–42.
23. Hsu JL, Huang SY, Chow NH, Chen SH. Stable-isotope dimethyl labeling for quantitative proteomics. Anal Chem 2003;75:6843–52.
24. Boersema PJ, Raijmakers R, Lemeer S, Mohammed S, Heck AJ. Multiplex peptide stable isotope dimethyl labeling for quantitative proteomics. Nat Protoc 2009;4:484–94.
25. Wiśniewski JR, Zougman A, Nagaraj N, Mann M. Universal sample preparation method for proteome analysis. Nat Methods 2009;6:359–62.

26. Kong RP, Siu SO, Lee SS, Lo C, Chu IK. Development of online high-/low-pH reversed-phase-reversed-phase two-dimensional liquid chromatography for shotgun proteomics: a reversed-phase-strong cation exchange-reversed-phase approach. J Chromatogr A 2011;1218:3681–8.
27. Bhat AA, Uppada S, Achkar IW, Hashem S, Yadav SK, Shanmugakonar M, et al. Tight junction proteins and signaling pathways in cancer and Inflammation: A functional crosstalk. Front Physiol 2018;9:1942.
28. R.TerBush D Maurice T, Roter D, Novick P. The exocyst is a multiprotein complex required for exocytosis in Saccharomyces cerevisiae. EMBO J 1996;15: 6483–94.
29. Sans N, Prybylowski K, Petralia RS, Chang K, Wang YX, Racca C, et al. NMDA receptor trafficking through an interaction between PDZ proteins and the exocyst complex. Nat Cell Biol 2003;5:520–30.
30. Tanaka T, Iino M. Sec8 regulates cytokeratin8 phosphorylation and cell migration by controlling the ERK and p38 MAPK signaling pathways. Cell Signal 2015; 27:1110–9.
31. Satow R, Nakamura T, Kato C, Endo M, Tamura M, Batori R, et al. ZIC5 drives melanoma aggressiveness by PDGFD-mediated activation of FAK and STAT3. Cancer Res 2017;77:366–77.
32. Nguyen K, Yan Y, Yuan B, Dasgupta A, Sun J, Mu H, et al. ST8SIA1 regulates tumor growth and metastasis in TNBC by activating the FAK-AKT-mTOR signaling pathway. Mol Cancer Ther 2018;17:2689–701.
33. Tanaka T, Iino M, Goto K. Knockdown of Sec6 improves cell–cell adhesion by increasing α-E-catenin in oral cancer cells. FEBS Lett 2012;586:924–33.
34. Zhang H, Schaefer A, Wang Y, Hodge RG, Blake DR, Diehl JN, et al. Gain-of-function RHOA mutations promote focal adhesion kinase activation and dependency in diffuse gastric cancer. Cancer Discov 2020;10:288–305.
35. Shen M, Jiang YZ, Wei Y, Ell B, Sheng X, Esposito M, et al. Tinagl1 suppresses triple-negative breast cancer progression and metastasis by simultaneously inhibiting Integrin/FAK and EGFR signaling. Cancer Cell 2019;35:64–80.
36. Kurmasheva RT, Gorlick R, Kolb EA, Keir ST, Maris JM, Lock RB, et al. Initial testing of VS-4718, a novel inhibitor of focal adhesion kinase (FAK), against pediatric tumor models by the Pediatric Preclinical Testing Program. Pediatr Blood Cancer 2017;64:10.
37. Ma D, Kou X, Jin J, Xu T, Wu M, Deng L, et al. Hydrostatic compress force enhances the viability and decreases the apoptosis of condylar chondrocytes through Integrin-FAK-ERK/PI3K pathway. Int J Mol Sci 2016;17:1847.
38. Lee BY, Timpson P, Horvath LG, Daly RJ. FAK signaling in human cancer as a target for therapeutics. Pharmacol Ther 2015;146:132–49.
39. Zhao X, Guan JL. Focal adhesion kinase and its signaling pathways in cell migration and angiogenesis. Adv Drug Deliv Rev 2011;63:610–5.
40. Yan HHN, Siu HC, Law S, Ho SL, Yue SSK, Tsui WY, et al. A comprehensive human gastric cancer organoid biobank captures tumor subtype heterogeneity and enables therapeutic screening. Cell Stem Cell 2018;23:882–97.
41. Shi XJ, Wei Y, Ji B. Systems biology of gastric cancer: perspectives on the omics-based diagnosis and treatment. Front Mol Biosci 2020;7:203.
42. Ge S, Xia X, Ding C, Zhen B, Zhou Q, Feng J, et al. A proteomic landscape of diffuse-type gastric cancer. Nat Commun 2018;9:1012.